Tenth-Order Lepton Anomalous Magnetic Moment—Sixth-Order Vertices Containing Vacuum-Polarization Subdiagrams

Tatsumi Aoyama, Masashi Hayakawa, Toichiro Kinoshita, and Makiko Nio

Phys. Rev. D **84**, 053003 — Published 6 September 2011

DOI: 10.1103/PhysRevD.84.053003

Tenth-Order Lepton Anomalous Magnetic Moment – Sixth-Order Vertices Containing Vacuum-Polarization Subdiagrams

Tatsumi Aoyama,[1,2] Masashi Hayakawa,[3,2] Toichiro Kinoshita,[4,2] and Makiko Nio[2]

[1]*Kobayashi-Maskawa Institute for the Origin of Particles and the Universe (KMI), Nagoya University, Nagoya, 464-8602, Japan*

[2]*Nishina Center, RIKEN, Wako, Japan 351-0198*

[3]*Department of Physics, Nagoya University, Nagoya, Japan 464-8602*

[4]*Laboratory for Elementary-Particle Physics, Cornell University, Ithaca, New York, 14853, U.S.A*

Abstract

This paper reports the values of contributions to the electron $g-2$ from 300 Feynman diagrams of the gauge-invariant Set III(a) and 450 Feynman diagrams of the gauge-invariant Set III(b). The evaluation is carried out in two versions. *Version A* is to start from the sixth-order magnetic anomaly M_6 obtained in the previous work. The mass-independent contributions of Set III(a) and Set III(b) are 2.1275 (2) and 3.3271 (6) in units of $(\alpha/\pi)^5$, respectively. *Version B* is based on the recently-developed automatic code generation scheme. This method yields 2.1271 (3) and 3.3271 (8) in units of $(\alpha/\pi)^5$, respectively. They are in excellent agreement with the results of the first method within the uncertainties of numerical integration. Combining these results as statistically independent we obtain the best values, 2.1273 (2), and 3.3271 (5) times $(\alpha/\pi)^5$, for the mass-independent contributions of the Set III(a) and Set III(b), respectively. We have also evaluated mass-dependent contributions of diagrams containing muon and/or tau-particle loop. Including them the total contribution of Set III(a) is 2.1349 (2) and that of Set III(b) is 3.3299 (5) in units of $(\alpha/\pi)^5$. The total contributions to the muon g–2 of various leptonic vacuum-polarization loops of Set III(a) and Set III(b) are 112.418 (32) and 15.407 (5) in units of $(\alpha/\pi)^5$, respectively.

PACS numbers: 13.40.Em,14.60.Cd,12.20.Ds,06.20.Jr

I. INTRODUCTION

The anomalous magnetic moment $g-2$ of the electron has played the central role in testing the validity of quantum electrodynamics (QED) as well as the Standard Model. The latest measurement of $a_e \equiv (g-2)/2$ by the Harvard group has reached the precision of 0.24×10^{-9} [1, 2]:

$$a_e(\mathrm{HV08}) = 1\ 159\ 652\ 180.73\ (0.28) \times 10^{-12} \quad [0.24\mathrm{ppb}]\ . \tag{1}$$

At present the theoretical prediction consists of QED corrections of up to the eighth order [3–5], and hadronic corrections [6–12] and electro-weak corrections [13–15] scaled down from their contributions to the muon $g-2$. To compare the theory with the measurement (1), we also need the value of the fine structure constant α determined by a method independent of $g-2$. The best value of such an α has been obtained recently from the measurement of h/m_{Rb}, the ratio of the Planck constant and the mass of Rb atom, combined with the very precisely known Rydberg constant and m_{Rb}/m_e: [16]

$$\alpha^{-1}(\mathrm{Rb10}) = 137.035\ 999\ 037\ (91) \quad [0.66\mathrm{ppb}]. \tag{2}$$

With this α the theoretical prediction of a_e becomes

$$a_e(\mathrm{theory}) = 1\ 159\ 652\ 181.13\ (0.11)(0.37)(0.77) \times 10^{-12}, \tag{3}$$

where the first, second, and third uncertainties come from the calculated eighth-order QED term, the tenth-order estimate, and the fine structure constant (2), respectively. The theory (3) is thus in good agreement with the experiment (1):

$$a_e(\mathrm{HV08}) - a_e(\mathrm{theory}) = -0.40\ (0.88) \times 10^{-12}, \tag{4}$$

proving that QED (Standard Model) is in good shape even at this very high precision.

An alternative test of QED is to compare $\alpha(\mathrm{Rb10})$ with the value of α determined from the experiment and theory of $g-2$:

$$\alpha^{-1}(a_e08) = 137.035\ 999\ 085\ (12)(37)(33) \quad [0.37\mathrm{ppb}], \tag{5}$$

where the first, second, and third uncertainties come from the eighth-order QED term, the tenth-order estimate, and the measurement of $a_e(\mathrm{HV08})$, respectively. Although the uncertainty of $\alpha^{-1}(a_e08)$ in (5) is a factor 2 smaller than $\alpha(\mathrm{Rb10})$, it is not a firm factor since it depends on the estimate of the tenth-order term, which is only a crude guess [17]. For a more stringent test of QED, it is obviously necessary to calculate the actual value of the tenth-order term. In anticipation of this challenge we launched a systematic program several years ago to evaluate the complete tenth-order term [18–20].

The 10th-order QED contribution to the anomalous magnetic moment of an electron can be written as

$$a_e^{(10)} = \left(\frac{\alpha}{\pi}\right)^5 \left[A_1^{(10)} + A_2^{(10)}(m_e/m_\mu) + A_2^{(10)}(m_e/m_\tau) + A_3^{(10)}(m_e/m_\mu, m_e/m_\tau)\right], \quad (6)$$

where $m_e/m_\mu = 4.836\ 331\ 71\ (12) \times 10^{-3}$ and $m_e/m_\tau = 2.875\ 64\ (47) \times 10^{-4}$ [17]. In the rest of this article the factor $\left(\frac{\alpha}{\pi}\right)^5$ will be suppressed for simplicity.

The contribution to the mass-independent term $A_1^{(10)}$ can be classified into six gauge-invariant sets, further divided into 32 gauge-invariant subsets depending on the nature of closed lepton loop subdiagrams. Thus far, numerical results of 27 gauge-invariant subsets, which consist of 3106 vertex diagrams, have been published [18, 21–26]. Five of these 27 subsets were also calculated analytically [27, 28]. Our calculation is in good agreement with the analytic results.

In this paper we report the evaluation of the tenth-order lepton $g-2$ from two gauge-invariant subsets called Set III(a) and Set III(b). These diagrams are built from the magnetic moment contribution M_6 (shown in Fig. 1) which consists of 50 proper sixth-order vertices of three-photon-exchange type, namely diagrams without closed lepton loops (and called q-type. See Ref. [4] for the definition of q-type.), by insertion of various lepton vacuum-polarization loops.

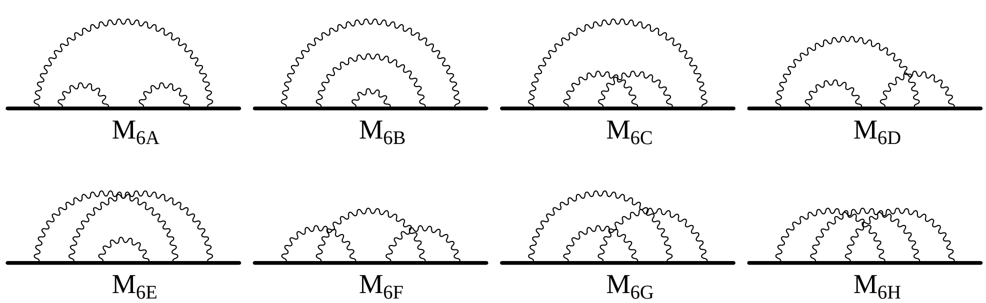

FIG. 1: The sixth-order q-type diagrams. The solid line represents the electron in a constant magnetic field. The time reversal diagrams of M_{6D} and M_{6G} are omitted for simplicity.

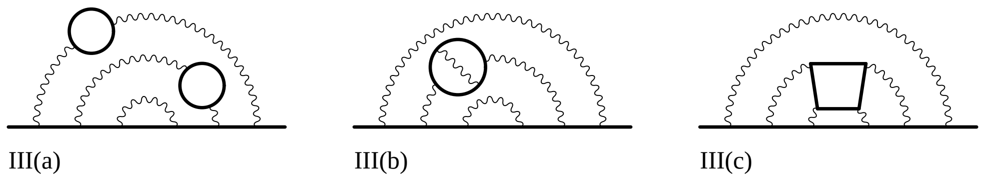

FIG. 2: Typical diagrams of Set III.

Set III(a). Diagrams obtained by inserting two second-order vacuum-polarization function Π_2's in M_6. The number of vertex diagrams contributing to $A_1^{(10)}$ is 300.

Set III(b). Diagrams obtained by inserting the fourth-order vacuum-polarization function Π_4 in M_6, where Π_4 is the sum of three fourth-order vacuum polarization loops. The number of vertex diagrams contributing to $A_1^{(10)}$ is 450.

Another set (Set III(c) of Fig. 2) consists of diagrams obtained by inserting a light-by-light scattering subdiagram Λ_4 in M_6. The total number of these diagrams contributing to $A_1^{(10)}$ is 390. Since it has a structure different from those of Sets III(a) and III(b), it will be treated in a separate paper.

Evaluation of Set III(a) and Set III(b) is carried out in two ways. *Version A* is to start from the FORTRAN code of the sixth-order anomalous magnetic moment M_6, which was obtained in previous works [29] and known to give the result identical with the analytic result [30]. It is thus easy to establish the validity of these FORTRAN codes for Sets III(a) and III(b).

We also evaluate these sets by an alternative method, *Version B*, using FORTRAN codes generated from scratch by the recently developed automatic code generation scheme [4, 19]. This approach deals with the UV renormalization as well as IR subtraction terms as integral parts of automation. In carrying out this automation scheme, we found it useful to construct IR subtraction terms in a different manner from that of *Version A* [19]. Thus, *Version B* provides an independent confirmation of *Version A*. At the same time it helps to verify the automated code generation scheme, which is developed primarily to deal with the vastly more difficult problem of Set V, which consists of 6354 vertex diagrams with pure radiative correction.

As is well-known, the insertion of vacuum-polarization loop such as $\Pi^{(2)}$ and $\Pi^{(4)}$ in an internal photon line of momentum q can be expressed as a superposition of massive vector

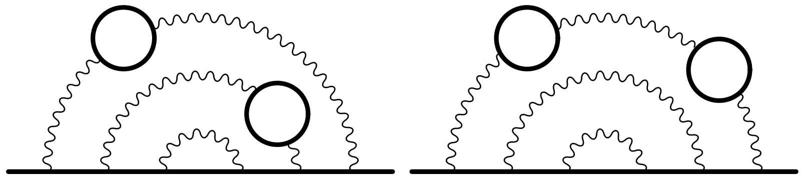

FIG. 3: Typical tenth-order diagrams of Set III(a) obtained by insertion of two second-order vacuum-polarization loops Π_2 in lepton diagrams of the three-photon-exchange type. The subset III(a_d) consists of diagrams in which Π_2 are inserted in different photon lines, while the subset III(a_s) consists of diagrams in which Π_2 are inserted in the same photon line. There are 150 diagrams in each subset.

propagators

$$\int_{4m^2}^{\infty} \frac{d\sigma \rho(\sigma)}{q^2 - \sigma}, \tag{7}$$

where m is the mass of the lepton forming the closed loop and σ is the square of mass of the vector particle and ρ is the spectral function. This enables us to obtain Feynman-parametric integrals for Set III(b) by simply replacing the relevant photon mass squared by σ and integrating over σ. It can also be applied to diagrams of Set III(a) which contain two vacuum-polarization loops in *different* photon lines. This subset of Set III(a) will be denoted as Set III(a_d) henceforth.

The Set III(a) also contains diagrams in which two vacuum-polarization loops are inserted in the *same* photon line, which will be denoted as Set III(a_s). For these diagrams a slight extension of Eq. (7) is required. When two vacuum polarization loops are inserted in a photon line of momentum q, the result, omitting integrations for simplicity, is given by the left-hand-side of the following equation, which can be rewritten in the form on the right-hand-side:

$$\frac{1}{q^2 - \sigma_a} q^2 \frac{1}{q^2 - \sigma_b} \equiv \frac{\sigma_a}{\sigma_a - \sigma_b} \frac{1}{q^2 - \sigma_a} - \frac{\sigma_b}{\sigma_a - \sigma_b} \frac{1}{q^2 - \sigma_b}. \tag{8}$$

Note that the right-hand-side is a linear combination of propagators of mass-square σ_a and σ_b with coefficients $\sigma_a/(\sigma_a - \sigma_b)$ and $-\sigma_b/(\sigma_a - \sigma_b)$. This enables us to write the Feynman-parametric integrals for the diagrams in Set III(a_s) by a simple extension of M_6 integrals. Eq. (8) can be readily extended to the case in which three or more vacuum-polarization loops are inserted in the same photon line.

These adaptations require a slight modification of the numerator function V, which, for M_6, is given by

$$
\begin{aligned}
V_0 &= \sum_{i=1}^{5} z_i(1-A_i)m_e^2, \\
V &= V_0 + (z_a+z_b+z_c)\lambda^2 \ , \qquad (9)
\end{aligned}
$$

where z_i $(i=1,\cdots,5)$, and z_j $(j=a,b,c)$ are Feynman parameters assigned to the fermion propagators and the photon propagators, respectively. m_e and λ are masses of the electron and photon, respectively. A_i $(i=1,\cdots,5)$ are *scalar currents* flowing in the fermion line i (see the exact definition of A_i in Ref. [29]). A_i is expressed by the Feynman parameters and its expression depends on the structure of a diagram. But, the expression of V in terms of A_i is identical for all diagrams of M_6.

When one vacuum-polarization function is inserted in a photon line, we must replace the mass square λ^2 of the photon in Eq. (9) by $p(t)$:

$$
\lambda^2 \longrightarrow p(t) \equiv \frac{4m_{vp}^2}{1-t^2}, \qquad (10)
$$

where m_{vp} is the rest mass of the fermion forming the vacuum-polarization loop and the interval $4m_{vp}^2 \leq \sigma < \infty$ of Eq. (7) is mapped onto $(0 \leq t < 1)$ for the sake of convenience.

When two vacuum-polarization functions are inserted in the same photon line a, it follows from Eq. (8) that the denominators must be modified as follows:

$$
\begin{aligned}
\frac{1}{V} &\longrightarrow \frac{V_0}{V_1V_2}, \\
\frac{1}{V^2} &\longrightarrow \frac{V_0^2 - z_a^2 p_1(t_1)p_2(t_2)}{(V_1V_2)^2}, \\
\frac{1}{V^3} &\longrightarrow \frac{V_0^3 - 3V_0 z_a^2 p_1(t_1)p_2(t_2) - z_a^3 p_1(t_1)p_2(t_2)(p_1(t_1)+p_2(t_2))}{(V_1V_2)^3} \ , \qquad (11)
\end{aligned}
$$

where

$$
V_i \equiv V_0 + z_a p_i(t_i) + (z_b+z_c)\lambda^2, \quad i=1,2, \qquad (12)
$$

for the first or second vacuum-polarization functions.

Throughout this article we use the exact renormalized forms of Π_2 and Π_4 instead of intermediately renormalized forms to take advantage of the known analytic forms of their spectral functions [31].

II. SET III(A)

Diagrams belonging to the Set III(a) are generated by inserting two second-order vacuum-polarization loops Π_2 in the photon lines of M_6. Using an identity derived from the Ward-Takahashi identity [18] and time-reversal invariance and summing up all possible insertions of the photon spectral function reduce the number of independent integrals from 300 to 16. For programming purpose it is convenient to treat Set III(a_d) and Set III(a_s) separately.

A. Set III(a_d)

Let $M_{6\alpha,P2P2}$ be the magnetic moment projection of the Set III(a_d) generated from a self-energy diagram $M_{6\alpha}$ (α =A through H) by insertion of two electron vacuum-polarization loops Π_2 in different photon lines (see Fig. 3). The subscript $P2P2$ implies that two second-order vacuum polarization function $P2$'s are inserted in different photon lines of the proper diagram $M_{6\alpha}$. To be precise $M_{6\alpha,P2P2}$ should be written as $M^{(l_1 l_2 l_3)}_{6\alpha,P2P2}$, where the first superscript l_1 refers to the open lepton line and l_2 and l_3 refer to closed lepton loops. When l_1, l_2, and l_3 are identical so that $M_{6\alpha,P2P2}$ is mass-independent, we omit the superscripts for simplicity. Distinction by superscript becomes necessary in Sec. II A 3 where mass-dependent terms are treated.

1. *Electron $g-2$: Version A*

In *Version A* the renormalized contribution of the diagrams of Set III(a_d) can be written as [32]

$$a_e^{(10)}[\text{Set III}(\mathrm{a}_d)] = \sum_{\alpha=A}^{H} a_{6\alpha,P2P2}, \tag{13}$$

with

$$a_{6\alpha,P2P2} = \Delta M_{6\alpha,P2P2} + \text{residual renormalization terms}, \tag{14}$$

where $\Delta M_{6\alpha,P2P2}$ is the UV- and IR-finite part of $M_{6\alpha,P2P2}$ after all divergences are removed by intermediate renormalization by K_S and I_R operations. See Ref. [32] for definitions of K-operation and I-operation.

When summed over all diagrams of Set III(a_d), the UV- and IR-divergent pieces cancel out and the total contribution to $a^{(10)}$ can be written as a sum of finite pieces [18]:

$$
\begin{aligned}
a_e^{(10)}[\text{Set III}(\text{a}_d) : \textit{Ver. A}] = & \sum_{\alpha=A}^{H} \Delta M_{6\alpha,P2P2} \\
& - 3\Delta B_{2,P2}\Delta M_{4,P2} - 3\Delta B_2 \Delta M_{4,P2P2} \\
& + \Delta\delta m_{4,P2}(M_{2^*,P2}[I] - M_{2^*,P2}) + \Delta\delta m_{4,P2P2}(M_{2^*}[I] - M_{2^*}) \\
& - [\Delta B_{4,P2} + 2\Delta L_{4,P2} - 4\Delta B_2 \Delta B_{2,P2}] M_{2,P2} \\
& - [\Delta B_{4,P2P2} + 2\Delta L_{4,P2P2} - 2(\Delta B_{2,P2})^2] M_2,
\end{aligned} \tag{15}
$$

where the number of vertex diagrams represented by $\Delta M_{6\alpha,P2P2}$ is 15 for $\alpha = A, B, C, E, F, H$ and 30 for $\alpha = D, G$ (see Fig. 1). We use the compactified notations for the magnetic moment, mass renormalization constant, wave-function renormalization constant, and vertex renormalization constants of fourth order [32]:

$$
\begin{aligned}
\Delta M_4 &\equiv \Delta M_{4a} + \Delta M_{4b}, \\
\Delta\delta m_4 &\equiv \Delta\delta m_{4a} + \Delta\delta m_{4b}, \\
\Delta B_4 &\equiv \Delta B_{4a} + \Delta B_{4b}, \\
\Delta L_4 &\equiv \sum_{i=1}^{3} (\Delta L_{4a,i} + \Delta L_{4b,i}),
\end{aligned} \tag{16}
$$

where $4a$ and $4b$ refer to fourth-order diagrams with two photons crossed and uncrossed, respectively, and $i = 1, 2, 3$ refers to three consecutive lepton lines of the diagram of type $4a$ or $4b$. M_{2^*} is the second-order magnetic moment with a two-point vertex insertion. $M_{2^*}[I]$ is the specific limit of M_{2^*} related to I-operation defined in Refs. [32, 33]. The subscript $P2$ in Eq. (15) means that a second-order vacuum-polarization function Π_2 is inserted in one of photon lines of the proper diagram in all possible ways. Similarly, $P2P2$ means that two Π_2's are inserted in two different photon lines in all possible ways.

The numerical values of $\Delta M_{6\alpha,P2P2}$ are summarized in Table I. Numerical values of auxiliary integrals needed to complete the renormalization are listed in Table II.

Substituting the values listed in Tables I and II into Eq. (15), we obtain

$$
a_e^{(10)}[\text{Set III}(\text{a}_d) : \textit{Ver. A}] = 0.941\ 92\ (7). \tag{17}
$$

TABLE I: Contributions of the Set III(a_d) diagrams to the electron $g-2$ evaluated in *Version A*. Both closed loops are electron loops. n_F is the number of Feynman diagrams represented by the integral. All integrals are evaluated in double precision. First 50 iterations are carried out using 1×10^8 sampling points per iteration. We then estimate how many more sampling points are needed to reach the desired precision. We chose 1×10^9 sampling points per iteration and iterated 50 more times.

Integral	n_F	Value (Error) including n_F	Sampling per iteration	No. of iterations
$\Delta M_{6A,P2P2}$	15	−0.108 564 (3)	$1 \times 10^8, 1 \times 10^9$	50,50
$\Delta M_{6B,P2P2}$	15	0.107 954 (11)	$1 \times 10^8, 1 \times 10^9$	50,50
$\Delta M_{6C,P2P2}$	15	0.193 333 (6)	$1 \times 10^8, 1 \times 10^9$	50,50
$\Delta M_{6D,P2P2}$	30	0.176 456 (20)	$1 \times 10^8, 1 \times 10^9$	50,50
$\Delta M_{6E,P2P2}$	15	0.142 839 (11)	$1 \times 10^8, 1 \times 10^9$	50,50
$\Delta M_{6F,P2P2}$	15	0.194 882 (15)	$1 \times 10^8, 1 \times 10^9$	50,50
$\Delta M_{6G,P2P2}$	30	0.542 183 (34)	$1 \times 10^8, 1 \times 10^9$	50,50
$\Delta M_{6H,P2P2}$	15	−0.190 026 (43)	$1 \times 10^8, 1 \times 10^9$	50,50

2. *Electron $g-2$: Version B*

The FORTRAN programs of *Version B* were generated by the automation code GENCODEN with slight modification. Given one-line information specifying a diagram, GENCODEN produces a set of programs for a q-type diagram of any order of the perturbation theory[19, 20]. The insertion of the vacuum polarization function in a photon line is a trivial task requiring modification of just a few lines of the GENCODEN source code. The K-operation method developed in Ref. [33] can be easily automated and incorporated in GENCODEN [19] to deal with UV divergence. IR divergence, on the other hand, is somewhat differently treated.

The I-operation defined in the previous work [32, 35] successfully generates the IR subtraction terms for a q-type diagram of up to the eighth-order of the perturbation theory. Actually, the I-operation works even for the tenth-order case, except that the automation becomes tremendously complicated. This is why we sought another way to handle the IR divergence. Namely, we deviated from the strict IR power counting, on which the I-operation

TABLE II: Auxiliary integrals for the Set III(a_d) and Set III(a_s) with $(l_1 l_2 l_3) = (eee)$, where $(l_1 l_2 l_3)$ is defined in II A. Six lines in the middle are for Set III (a_d) and bottom four lines are for Set III (a_s). Some integrals are known exactly. Other integrals are obtained by VEGAS integration [34].

Integral	Value(Error)	Integral	Value(Error)
M_2	0.5	M_{2^*}	1.0
$M_{2^*}[I]$	-1.0	ΔB_2	0.75
ΔM_4	0.030 833 612...	$\Delta\delta m_4$	1.906 340 (21)
ΔL_4	0.465 024 (17)	ΔB_4	-0.437 094 (21)
$M_{2,P2}$	0.015 687 421...	$M_{2^*,P2}$	0.044 077 4 (3)
$M_{2^*,P2}[I]$	0.010 255 3 (11)	$\Delta M_{4,P2}$	-0.106 707 082...
$\Delta B_{2,P2}$	0.063 399 266...	$\Delta\delta m_{4,P2}$	0.679 769 (15)
$\Delta L_{4,P2}$	0.200 092 (14)	$\Delta B_{4,P2}$	-0.314 320 (10)
$\Delta M_{4,P2P2}$	-0.026 682 (2)	$\Delta\delta m_{4,P2P2}$	0.105 075 (11)
$\Delta L_{4,P2P2}$	0.005 481 (8)	$\Delta B_{4,P2P2}$	-0.071 017 (4)
$M_{2,P2:2}$	0.002 558 524...	$M_{2^*,P2:2}$	0.008 482 (1)
$M_{2^*,P2:2}[I]$	0.032 904 (9)	$\Delta M_{4,P2:2}$	-0.057 587 8 (9)
$\Delta B_{2,P2:2}$	0.027 902 3 (4)	$\Delta\delta m_{4,P2:2}$	0.439 326 (81)
$\Delta L_{4,P2:2}$	0.094 940 (26)	$\Delta B_{4,P2:2}$	-0.199 173 (89)

is defined, and took a more diagrammatic approach.

The new scheme to deal with the IR divergence, called I/R-subtraction, consists of two parts: One is the R-subtraction that removes the UV-finite part of mass-renormalization term, which is the cause of linear IR divergence. (The UV-divergent part of the mass renormalization is removed by the K-operation.) Once the mass renormalization is completed, the remaining IR divergence is only logarithmic and is easily subtracted by the second part called I-subtraction. This I-subtraction is similar to the previous I-operation, except that it uses the finite part of a vertex renormalization constant in addition to the logarithmic IR-divergent part as an IR-counter term. The I/R-subtraction can be readily incorporated in GENCODEN [20].

As far as the sixth-order diagrams are concerned, two methods of IR treatment, I-

operation or I/R-subtraction, work fine making no significant difference. The difference is only finite amount in the amplitude of the magnetic moments, which can be identified analytically. Taking it into account, we obtain the relation of the magnetic moment amplitudes in *Version A* and *Version B* as follows:

$$\begin{aligned}
\Delta M^{(B)}_{6A,P2P2} &= \Delta M^{(A)}_{6A,P2P2} - 2\Delta L_{4b,1,P2} M_{2,P2} - 2\Delta L_{4b,1,P2P2} M_2, \\
\Delta M^{(B)}_{6B,P2P2} &= \Delta M^{(A)}_{6B,P2P2} - \Delta L_{4b,2,P2} M_{2,P2} - \Delta L_{4b,2,P2P2} M_2 \\
&- \Delta\delta m_{4b,P2}(M_{2^*P2} - M_{2^*P2}[I]) - \Delta\delta m_{4b,P2P2}(M_{2^*} - M_{2^*}[I]), \\
\Delta M^{(B)}_{6C,P2P2} &= \Delta M^{(A)}_{6C,P2P2} - \Delta\delta m_{4a,P2}(M_{2^*P2} - M_{2^*P2}[I]) \\
&- \Delta\delta m_{4a,P2P2}(M_{2^*} - M_{2^*}[I]), \\
\Delta M^{(B)}_{6D,P2P2} &= \Delta M^{(A)}_{6D,P2P2} - 2\Delta L_{4a,1,P2} M_{2,P2} - 2\Delta L_{4a,1,P2P2} M_2, \\
\Delta M^{(B)}_{6E,P2P2} &= \Delta M^{(A)}_{6E,P2P2} - \Delta L_{4a,2,P2} M_{2,P2} - \Delta L_{4a,2,P2P2} M_2, \\
\Delta M^{(B)}_{6F,P2P2} &= \Delta M^{(A)}_{6F,P2P2}, \\
\Delta M^{(B)}_{6G,P2P2} &= \Delta M^{(A)}_{6G,P2P2}, \\
\Delta M^{(B)}_{6H,P2P2} &= \Delta M^{(A)}_{6H,P2P2}.
\end{aligned} \tag{18}$$

Note that the *Version B* of $\Delta M_{6\alpha,P2P2}$ absorbs not only $\Delta\delta m$ terms but also part of ΔL_4 terms. From Eqs. (15) and (18) we obtain

$$\begin{aligned}
a_e^{(10)}[\text{Set III}(\mathrm{a}_d) : \textit{Ver. B}] = \sum_{\alpha=A}^{H} \Delta M^{(B)}_{6\alpha,P2P2} \\
&- 3\Delta B_{2,P2}\Delta M_{4,P2} - 3\Delta B_2 \Delta M_{4,P2P2} \\
&- [\Delta B_{4,P2} + \Delta L_{4,P2} - 4\Delta B_2 \Delta B_{2,P2}] M_{2,P2} \\
&- (\Delta B_{4,P2P2} + \Delta L_{4,P2P2} - 2(\Delta B_{2,P2})^2) M_2.
\end{aligned} \tag{19}$$

Of course this shift of terms in Eq. (15) does not affect the final result.

This is a trivial change for the Set III. However, in Set V, which consists entirely of q-type tenth-order diagrams, residual renormalization terms of $\Delta\delta m$ type give rise to linear IR-divergences which complicate the analysis of the renormalization scheme. Thus there is an advantage in removing the self-mass terms completely, not just their UV-divergent parts.

Substituting the values listed in Tables II and III in Eq. (19), we obtain

$$a_e^{(10)}[\text{Set III}(\mathrm{a}_d) : \textit{Ver. B}] = 0.941\ 81\ (12), \tag{20}$$

which is in good agreement with (17).

TABLE III: *Version B* contributions of the Set III(a_d) diagrams to the electron $g-2$. The corresponding programs are created by GENCODEN. Both closed loops are electron loops. n_F is the number of Feynman diagrams represented by the integral. All integrals are evaluated in double precision.

Integral	n_F	Value (Error) including n_F	Sampling per iteration	No. of iterations
$\Delta M_{6A,P2P2}$	15	−0.130 613 (29)	1×10^8	700
$\Delta M_{6B,P2P2}$	15	−0.031 263 (26)	1×10^8	700
$\Delta M_{6C,P2P2}$	15	0.080 981 (24)	1×10^8	700
$\Delta M_{6D,P2P2}$	30	0.170 496 (41)	1×10^8	700
$\Delta M_{6E,P2P2}$	15	0.183 485 (29)	1×10^8	700
$\Delta M_{6F,P2P2}$	15	0.194 756 (31)	1×10^8	700
$\Delta M_{6G,P2P2}$	30	0.541 900 (69)	1×10^8	700
$\Delta M_{6H,P2P2}$	15	−0.189 816 (54)	1×10^8	700

3. Mass-dependent terms A_2 and A_3 of Set III(a_d)

Once FORTRAN programs for mass-independent Set III(a_d) diagrams are obtained, it is straightforward to evaluate contributions of mass-dependent term $A_2^{(10)}(m_e/m_\mu)$, $A_2^{(10)}(m_e/m_\tau)$, and $A_3^{(10)}(m_e/m_\mu, m_e/m_\tau)$. We just have to choose an appropriate fermion mass m_{vp} in Eq. (10). Obviously the residual renormalization terms of Set III(a_d) are slightly more complicated because of insertions of vacuum-polarization loops in several photon lines. Note also that the integrands of these sets may be strongly peaked because of their dependence on $(m_e/m_\mu)^2$ or $(m_e/m_\tau)^2$ which makes them more susceptible to the digit deficiency problem.

Of course we can evaluate them by either *Version A* or *Version B*. Since we have established their equivalence, we may choose either one, say *Version A*.

In the general case ($l_1 l_2 l_3$), where $l_2 \neq l_3$, the residual renormalization terms of Set III(a_d)

in *Version A* have the form

$$
\begin{aligned}
a_e^{(10)}[\text{Set III}(\mathrm{a}_d)^{(l_1l_2l_3)}] = & \sum_{\alpha=A}^{H} \Delta M_{6\alpha,P2P2}^{(l_1l_2l_3)} \\
& - 3\Delta B_{2,P2}^{(l_1l_2)}\Delta M_{4,P2}^{(l_1l_3)} - 3\Delta B_{2,P2}^{(l_1l_3)}\Delta M_{4,P2}^{(l_1l_2)} - 3\Delta B_2 \Delta M_{4,P2P2}^{(l_1l_2l_3)} \\
& + \Delta\delta m_{4,P2}^{(l_1l_3)}(M_{2^*,P2}^{(l_1l_2)}[I] - M_{2^*,P2}^{(l_1l_2)}) + \Delta\delta m_{4,P2}^{(l_1l_2)}(M_{2^*,P2}^{(l_1l_3)}[I] - M_{2^*,P2}^{(l_1l_3)}) \\
& + \Delta\delta m_{4,P2P2}^{(l_1l_2l_3)}(M_{2^*}[I] - M_{2^*}) \\
& - [\Delta B_{4,P2}^{(l_1l_2)} + 2\Delta L_{4,P2}^{(l_1l_2)} - 4\Delta B_2 \Delta B_{2,P2}^{(l_1l_2)}] M_{2,P2}^{(l_1l_3)} \\
& - [\Delta B_{4,P2}^{(l_1l_3)} + 2\Delta L_{4,P2}^{(l_1l_3)} - 4\Delta B_2 \Delta B_{2,P2}^{(l_1l_3)}] M_{2,P2}^{(l_1l_2)} \\
& - [\Delta B_{4,P2P2}^{(l_1l_2l_3)} + 2\Delta L_{4,P2P2}^{(l_1l_2l_3)} - 4(\Delta B_{2,P2}^{(l_1l_3)}\Delta B_{2,P2}^{(l_1l_2)})] M_2.
\end{aligned} \tag{21}
$$

For instance, for $(l_1l_2l_3) = (eem)$, the first, second, and third symbols refer to the open electron line, electron loop, and muon loop, respectively. Some superscripts are denoted as (l_1l_2) or (l_1l_3) since they have only one internal loop. Superscripts (l_1) on $\Delta B_2, M_2$, etc., are omitted for simplicity since these terms are mass-independent. Note also that the second and third loops appear interchangeably in the case of Set III(a). Thus Eq. (21) represents the sum of (eem) and (eme).

If l_2 and l_3 represent identical particles, duplicate terms of Eq. (21) must be dropped to avoid double counting.

Substituting the values listed in Tables IV and XI into Eq. (21), we obtain

$$a_e^{(10)}[\text{Set III}(\mathrm{a}_d)^{(eem)}] = 0.003\ 166\ (4). \tag{22}$$

The contributions of diagrams of (eet), (emm), etc., can be calculate by just changing the mass parameters in FORTRAN programs. The residual renormalization can be carried out using Eq. (21) paying attention to whether $l_2 = l_3$ or not. We present the final results without giving details:

$$a_e^{(10)}[\text{Set III}(\mathrm{a}_d)^{(eet)}] = 0.000\ 031\ 55\ (8), \tag{23}$$

$$a_e^{(10)}[\text{Set III}(\mathrm{a}_d)^{(emm)}] = 0.000\ 080\ 45\ (11), \tag{24}$$

$$a_e^{(10)}[\text{Set III}(\mathrm{a}_d)^{(emt)}] = 0.000\ 005\ 56\ (2). \tag{25}$$

These results have been confirmed by comparison with the results of *Version B*.

The trend of mass dependence of these results indicates clearly that (ett) case will be an order of magnitude smaller than (25). Thus it may be ignored at present.

TABLE IV: Mass-dependent contributions of the Set III(a_d) diagrams to the electron g–2 evaluated in *Version A*. One closed loop is electron loop and the other is muon loop. Each integral is the sum of (eem) and (eme) types. n_F is the number of Feynman diagrams represented by the integral. All integrals are evaluated in double precision.

Integral	n_F	Value (Error) including n_F	Sampling per iteration	No. of iterations
$\Delta M^{(eem)}_{6A,P2P2}$	30	$-0.000\ 324\ (\ 1)$	1×10^7	20
$\Delta M^{(eem)}_{6B,P2P2}$	30	$0.000\ 357\ (\ 2)$	1×10^7	20
$\Delta M^{(eem)}_{6C,P2P2}$	30	$0.000\ 496\ (\ 1)$	1×10^7	20
$\Delta M^{(eem)}_{6D,P2P2}$	60	$0.000\ 533\ (\ 3)$	1×10^7	20
$\Delta M^{(eem)}_{6E,P2P2}$	30	$0.000\ 316\ (\ 2)$	1×10^7	20
$\Delta M^{(eem)}_{6F,P2P2}$	30	$0.000\ 659\ (\ 3)$	1×10^7	40
$\Delta M^{(eem)}_{6G,P2P2}$	60	$0.001\ 657\ (12)$	1×10^7	60
$\Delta M^{(eem)}_{6H,P2P2}$	30	$-0.000\ 313\ (12)$	1×10^7	20

4. Muon $g-2$. Set III(a_d)

The leading contribution to the muon $g-2$ comes from the (mee) case where both loops consist of electrons, and m stands for the open muon line. Results of numerical evaluation in *Version A* are listed in Table V. From this Table and Table VI we obtain

$$a_\mu^{(10)}[\text{Set III}(\mathrm{a}_d)^{(mee)}] = 42.460\ 4\ (188). \tag{26}$$

Next largest contribution comes from (mme). We list only the result:

$$a_\mu^{(10)}[\text{Set III}(\mathrm{a}_d)^{(mme)}] = 11.416\ 9\ (22). \tag{27}$$

We also obtained

$$a_\mu^{(10)}[\text{Set III}(\mathrm{a}_d)^{(met)}] = 0.421\ 97\ (19), \tag{28}$$

$$a_\mu^{(10)}[\text{Set III}(\mathrm{a}_d)^{(mmt)}] = 0.110\ 71\ (1), \tag{29}$$

$$a_\mu^{(10)}[\text{Set III}(\mathrm{a}_d)^{(mtt)}] = 0.008\ 50\ (10). \tag{30}$$

These results are in good agreement with the results of *Version B*.

TABLE V: Contributions of the Set III(a_d) diagrams to the muon $g-2$ evaluated in *Version A*. Both closed loops are electron loops. n_F is the number of Feynman diagrams represented by the integral. All integrals are evaluated in real(10) arithmetic build in *gfortran* to take advantage of the extended-precision format of a processor. This reduces possible *digit-deficiency* problem [36] substantially and runs much faster than software-implemented real(16) arithmetic.

Integral	n_F	Value (Error) including n_F	Sampling per iteration	No. of iterations
$\Delta M^{(mee)}_{6A,P2P2}$	15	$-35.558\ 8$ (48)	$1\times10^7, 4\times10^7$	20, 180
$\Delta M^{(mee)}_{6B,P2P2}$	15	44.427 6 (68)	$1\times10^7, 4\times10^7$	20, 180
$\Delta M^{(mee)}_{6C,P2P2}$	15	19.208 7 (65)	$1\times10^7, 4\times10^7$	20, 180
$\Delta M^{(mee)}_{6D,P2P2}$	30	28.117 1 (70)	$1\times10^7, 4\times10^7$	20, 280
$\Delta M^{(mee)}_{6E,P2P2}$	15	30.980 7 (64)	$1\times10^7, 4\times10^7$	20, 80
$\Delta M^{(mee)}_{6F,P2P2}$	15	18.790 9 (60)	$1\times10^7, 4\times10^7$	20, 180
$\Delta M^{(mee)}_{6g,P2P2}$	30	58.890 0 (71)	$1\times10^7, 4\times10^7$	20, 180
$\Delta M^{(mee)}_{6h,P2P2}$	15	$-51.550\ 0$ (70)	$1\times10^7, 4\times10^7$	20, 280

TABLE VI: Auxiliary integrals for Set III(a_d) and Set III(a_s), where $(l_1l_2l_3) = (mee)$. $M^{(me)}_{2,P2}$ and $M^{(mee)}_{2,P2:2}$ are known exactly[37–39] and their uncertainties are due to the uncertainty of the measured electron-muon mass ratio only. Other integrals are obtained by VEGAS integration [34].

Integral	Value(Error)	Integral	Value(Error)
$M^{(me)}_{2,P2}$	1.094 258 3086 (80)	$M^{(me)}_{2^*,P2}$	2.349 75 (29)
$M^{(me)}_{2^*,P2}[I]$	$-2.183\ 21$ (16)	$\Delta B^{(me)}_{2,P2}$	1.885 733 (16)
$\Delta\delta m^{(me)}_{4,P2}$	11.151 07 (49)	$\Delta M^{(me)}_{4,P2}$	$-0.628\ 831\ 80$ (2)
$\Delta L^{(me)}_{4,P2}$	3.119 86 (66)	$\Delta B^{(me)}_{4,P2}$	$-3.427\ 88$ (49)
$\Delta M^{(mee)}_{4,P2P2}$	$-1.959\ 37$ (30)	$\Delta\delta m^{(mee)}_{4,P2P2}$	16.575 79 (52)
$\Delta L^{(mee)}_{4,P2P2}$	4.960 40 (63)	$\Delta B^{(mee)}_{4,P2P2}$	$-6.353\ 75$ (62)
$M^{(mee)}_{2,P2:2}$	2.718 655 851 (82)	$M^{(mee)}_{2^*,P2:2}$	6.162 33 (39)
$M^{(mee)}_{2^*,P2:2}[I]$	$-5.107\ 35$ (28)	$\Delta B^{(mee)}_{2,P2:2}$	5.330 35 (12)
$\Delta M^{(mee)}_{4,P2:2}$	$-3.484\ 52$ (83)	$\Delta\delta m^{(mee)}_{4,P2:2}$	35.742 2 (12)
$\Delta L^{(mee)}_{4,P2:2}$	10.621 5 (13)	$\Delta B^{(mee)}_{4,P2:2}$	$-12.811\ 9$ (12)

B. Set III(a_s)

1. *Electron* $g-2$*. Version A*

Let $M_{6\alpha,P2:2}$ be the magnetic moment projection of the Set III(a_s) generated from self-energy-like diagrams 6α (α =A through H) by insertion of two Π_2's in the same photon line (see Fig. 3). The renormalized contribution due to these diagrams can be written in a way similar to Eq. (13).

When summed over all the diagrams of Set III(a_s), the UV- and IR-divergent pieces cancel out and the total contribution to $a^{(10)}$ can be written in *Version A* as a sum of finite pieces (which is similar to Eq. (5.39) of Ref. [32]):

$$\begin{aligned} a_e^{(10)}[\text{Set III}(\mathrm{a}_s) : \textit{Ver. A}] = & \sum_{\alpha=A}^{H} \Delta M_{6\alpha,P2:2} \\ & - 3\Delta B_{2,P2:2}\Delta M_4 - 3\Delta B_2 \Delta M_{4,P2:2} \\ & + \Delta\delta m_4 (M_{2^*,P2:2}[I] - M_{2^*,P2:2}) + \Delta\delta m_{4,P2:2}(M_{2^*}[I] - M_{2^*}) \\ & - [\Delta B_4 + 2\Delta L_4 - 2(\Delta B_2)^2] M_{2,P2:2} \\ & - [\Delta B_{4,P2:2} + 2\Delta L_{4,P2:2} - 4\Delta B_2 \Delta B_{2,P2:2}] M_2. \end{aligned} \tag{31}$$

The numerical values of $\Delta M_{6\alpha,P2:2}$ are summarized in Table VII. Numerical values of auxiliary integrals needed to complete the renormalization are listed in Table II.

Substituting the values listed in Tables II and VII into Eq. (31), we obtain

$$a_e^{(10)}[\text{Set III}(\mathrm{a}_s) : \textit{Ver. A}] = 1.185\ 56\ (20). \tag{32}$$

2. *Electron* $g-2$*. Version B*

For the reason discussed in Sec. II A 2 we obtain in *Version B* a formula for $a_e^{(10)}$[Set III(a_s)] which is different from (31):

$$\begin{aligned} a_e^{(10)}[\text{Set III}(\mathrm{a}_s) : \textit{Ver. B}] = & \sum_{\alpha=A}^{H} \Delta M^{(B)}_{6\alpha,P2:2} \\ & - 3\Delta B_{2,P2:2}\Delta M_4 - 3\Delta B_2 \Delta M_{4,P2:2} \\ & - [\Delta B_4 + \Delta L_4 - 2(\Delta B_2)^2] M_{2,P2:2} \\ & - (\Delta B_{4,P2:2} + \Delta L_{4,P2:2} - 4\Delta B_{2,P2:2}\Delta B_2) M_2, \end{aligned} \tag{33}$$

TABLE VII: *Version A* contributions of Set III(a_s) diagrams to the electron g–2. n_F is the number of Feynman diagrams represented by the integral. All integrals are evaluated in double precision.

Integral	n_F	Value (Error) including n_F	Sampling per iteration	No. of iterations
$\Delta M_{6A,P2:2}$	15	−0.204 682 (54)	$1\times10^8, 1\times10^9$	50,50
$\Delta M_{6B,P2:2}$	15	0.413 110 (56)	$1\times10^8, 1\times10^9$	50,50
$\Delta M_{6C,P2:2}$	15	0.458 938 (53)	$1\times10^8, 1\times10^9$	50,50
$\Delta M_{6D,P2:2}$	30	0.281 276 (54)	$1\times10^8, 1\times10^9$	50,50
$\Delta M_{6E,P2:2}$	15	0.220 637 (23)	$1\times10^8, 1\times10^9$	50,50
$\Delta M_{6F,P2:2}$	15	0.317 657 (48)	$1\times10^8, 1\times10^9$	50,50
$\Delta M_{6G,P2:2}$	30	0.765 073 (87)	$1\times10^8, 1\times10^9$	50,50
$\Delta M_{6H,P2:2}$	15	−0.409 439 (98)	$1\times10^8, 1\times10^9$	50,50

where

$$\begin{aligned}
\Delta M^{(B)}_{6A,P2:2} &= \Delta M^{(A)}_{6A,P2:2} - 2\Delta L_{4b,1} M_{2,P2:2} - 2\Delta L_{4b,1,P2:2} M_2, \\
\Delta M^{(B)}_{6B,P2:2} &= \Delta M^{(A)}_{6B,P2:2} - \Delta L_{4b,2} M_{2,P2:2} - \Delta L_{4b,2,P2:2} M_2 \\
&- \Delta\delta m_{4b}(M_{2^*P2:2} - M_{2^*P2:2}[I]) - \Delta\delta m_{4b,P2:2}(M_{2^*} - M_{2^*}[I]), \\
\Delta M^{(B)}_{6C,P2:2} &= \Delta M^{(A)}_{6C,P2:2} - \Delta\delta m_{4a}(M_{2^*P2:2} - M_{2^*P2:2}[I]) \\
&- \Delta\delta m_{4a,P2:2}(M_{2^*} - M_{2^*}[I]), \\
\Delta M^{(B)}_{6D,P2:2} &= \Delta M^{(A)}_{6D,P2:2} - 2\Delta L_{4a,1} M_{2,P2:2} - 2\Delta L_{4a,1,P2:2} M_2, \\
\Delta M^{(B)}_{6E,P2:2} &= \Delta M^{(A)}_{6E,P2:2} - \Delta L_{4a,2} M_{2,P2:2} - \Delta L_{4a,2,P2:2} M_2, \\
\Delta M^{(B)}_{6F,P2:2} &= \Delta M^{(A)}_{6F,P2:2}, \\
\Delta M^{(B)}_{6G,P2:2} &= \Delta M^{(A)}_{6G,P2:2}, \\
\Delta M^{(B)}_{6H,P2:2} &= \Delta M^{(A)}_{6H,P2:2}.
\end{aligned} \tag{34}$$

From Tables II and VIII we obtain

$$a_e^{(10)}[\text{Set III}(\text{a}_s) : \textit{Ver. B}] = 1.185\ 26\ (24), \tag{35}$$

in good agreement with (32).

TABLE VIII: *Version B* contributions of Set III(a_s) diagrams to the electron $g-2$. Programs are created by GENCODEN. n_F is the number of Feynman diagrams represented by the integral. All integrals are evaluated in double precision.

Integral	n_F	Value (Error) including n_F	Sampling per iteration	No. of iterations
$\Delta M_{6A,P2:2}$	15	−0.280 605 (31)	1×10^8	600
$\Delta M_{6B,P2:2}$	15	−0.068 830 (70)	1×10^8	600
$\Delta M_{6C,P2:2}$	15	0.070 002 (67)	1×10^8	600
$\Delta M_{6D,P2:2}$	30	0.269 937 (106)	1×10^8	600
$\Delta M_{6E,P2:2}$	15	0.297 943 (60)	1×10^8	600
$\Delta M_{6F,P2:2}$	15	0.317 432 (69)	1×10^8	600
$\Delta M_{6G,P2:2}$	30	0.764 711 (127)	1×10^8	600
$\Delta M_{6H,P2:2}$	15	−0.409 110 (103)	1×10^8	600

3. *Mass-dependent terms A_2 and A_3 of Set III(a_s)*

For the Set III(a_s) we have (in *Version A*)

$$\begin{aligned}
a_e^{(10)}[\text{Set III}(\mathrm{a}_s)^{(l_1l_2l_3)}] = &\sum_{\alpha=A}^{H} \Delta M_{6\alpha,P2:2}^{(l_1l_2l_3)} \\
&- 3\Delta B_{2,P2:2}^{(l_1l_2l_3)} \Delta M_4 - 3\Delta B_2 \Delta M_{4,P2:2}^{(l_1l_2l_3)} \\
&+ \Delta\delta m_4 (M_{2^*,P2:2}[I]^{(l_1l_2l_3)} - M_{2^*,P2:2}^{(l_1l_2l_3)}) + \Delta\delta m_{4,P2:2}^{(l_1l_2l_3)} (M_{2^*}[I] - M_{2^*}) \\
&- [\Delta B_4 + 2\Delta L_4 - 2(\Delta B_2)^2] M_{2,P2:2}^{(l_1l_2l_3)} \\
&- [\Delta B_{4,P2:2}^{(l_1l_2l_3)} + 2\Delta L_{4,P2:2}^{(l_1l_2l_3)} - 4\Delta B_2 \Delta B_{2,P2:2}^{(l_1l_2l_3)}] M_2.
\end{aligned} \tag{36}$$

Substituting the values listed in Tables IX and XI into Eq. (36), we obtain

$$a_e^{(10)}[\text{Set III}(\mathrm{a}_s)^{(eem)}] = 0.004\ 12\ (10). \tag{37}$$

We also obtained

$$\begin{aligned}
a_e^{(10)}[\text{Set III}(\mathrm{a}_s)^{(emm)}] &= 0.000\ 144\ 7\ (9), &(38)\\
a_e^{(10)}[\text{Set III}(\mathrm{a}_s)^{(eet)}] &= 0.000\ 045\ 95\ (23), &(39)\\
a_e^{(10)}[\text{Set III}(\mathrm{a}_s)^{(emt)}] &= 0.000\ 009\ 88\ (8). &(40)
\end{aligned}$$

TABLE IX: Contributions of diagrams of Set III(a_s) containing one electron vacuum-polarization loop and one muon vacuum-polarization loop. n_F is the number of Feynman diagrams represented by the integral. All integrals are evaluated in double precision.

Integral	n_F	Value (Error) including n_F	Sampling per iteration	No. of iterations
$\Delta M^{(eem)}_{6A,P2:2}$	30	−0.000 541 (4)	1×10^7	20
$\Delta M^{(eem)}_{6B,P2:2}$	30	0.001 434 (17)	1×10^7	20
$\Delta M^{(eem)}_{6C,P2:2}$	30	0.001 334 (26)	1×10^7	20
$\Delta M^{(eem)}_{6D,P2:2}$	60	0.000 747 (26)	1×10^7	20
$\Delta M^{(eem)}_{6E,P2:2}$	30	0.000 494 (10)	1×10^7	20
$\Delta M^{(eem)}_{6F,P2:2}$	30	0.001 233 (16)	1×10^7	20
$\Delta M^{(eem)}_{6G,P2:2}$	60	0.002 397 (78)	1×10^7	20
$\Delta M^{(eem)}_{6H,P2:2}$	30	−0.000 995 (43)	1×10^7	20

TABLE X: Contributions of the Set III(a_s) diagrams to the muon $g-2$ evaluated in *Version A*. Both closed loops are electron loops. n_F is the number of Feynman diagrams represented by the integral. All integrals are evaluated using real(10) arithmetic built in *gfortran*.

Integral	n_F	Value (Error) including n_F	Sampling per iteration	No. of iterations
$\Delta M^{(mee)}_{6A,P2P2}$	15	−38.157 8 (106)	$1 \times 10^7, 4 \times 10^7$	20, 80
$\Delta M^{(mee)}_{6B,P2P2}$	15	51.107 5 (103)	$1 \times 10^7, 4 \times 10^7$	20, 180
$\Delta M^{(mee)}_{6C,P2P2}$	15	20.547 7 (113)	$1 \times 10^7, 4 \times 10^7$	20, 180
$\Delta M^{(mee)}_{6D,P2P2}$	30	31.469 8 (113)	$1 \times 10^7, 4 \times 10^7$	20, 280
$\Delta M^{(mee)}_{6E,P2P2}$	15	32.799 0 (89)	$1 \times 10^7, 4 \times 10^7$	20, 80
$\Delta M^{(mee)}_{6F,P2P2}$	15	19.014 4 (96)	$1 \times 10^7, 4 \times 10^7$	20, 180
$\Delta M^{(mee)}_{6G,P2P2}$	30	61.519 4 (101)	$1 \times 10^7, 4 \times 10^7$	20, 180
$\Delta M^{(mee)}_{6H,P2P2}$	15	−55.142 4 (95)	$1 \times 10^7, 4 \times 10^7$	20, 280

These results are in good agreement with those of *Version B*. The contribution of the (ett) term is negligibly small.

TABLE XI: Auxiliary integrals which depend on the mass ratio m_μ/m_e. Those for Set III(a$_d$) are listed on the left side. Those for Set III(a$_s$) are listed on the top half of the right side. Those for Set III(b) are listed on the bottom half of the right side.

Integral	Value(Error)	Integral	Value(Error)
$\Delta M_{4,P2}^{(em)}$	−0.000 018 9 (1)	$\Delta M_{4,P2:2}^{(eem)}$	−0.000 074 7 (1)
$\Delta M_{4,P2P2}^{(eem)}$	−0.000 019 1 (1)	$M_{2^*,P2:2}^{(eem)}$	0.000 000 9 (0)
$M_{2,P2}^{(em)}$	0.015 690 0 (16)	$M_{2^*,P2:2}[I]^{(eem)}$	0.000 069 7 (1)
$M_{2^*,P2}^{(em)}$	0.044 089 4 (101)	$\Delta B_{2,P2:2}^{(eem)}$	0.000 036 2 (1)
$M_{2^*,P2}[I]^{(em)}$	0.010 274 2 (256)	$\Delta B_{4,P2:2}^{(eem)}$	−0.000 409 7 (48)
$\Delta B_{2,P2}^{(em)}$	0.000 009 4 (00)	$\Delta L_{4,P2:2}^{(eem)}$	0.000 016 0 (59)
$\Delta B_{4,P2}^{(em)}$	−0.000 091 5 (4)	$\Delta\delta m_{4,P2:2}^{(eem)}$	0.001 261 2 (63)
$\Delta L_{4,P2}^{(em)}$	0.000 012 7 (6)		
$\Delta B_{4,P2P2}^{(eem)}$	−0.000 129 0 (3)	$\Delta M_{4,P4}^{(em)}$	−0.000 068 2 (7)
$\Delta L_{4,P2P2}^{(eem)}$	−0.000 113 6 (6)	$M_{2^*,P4}^{(em)}$	0.000 005 9 (0)
$\Delta\delta m_{4,P2}^{(em)}$	0.000 253 9 (5)	$M_{2^*,P4}[I]^{(em)}$	0.000 052 0 (1)
$\Delta\delta m_{4,P2P2}^{(eem)}$	0.000 195 1 (3)	$\Delta B_{4,P4}^{(em)}$	−0.000 322 0 (9)
		$\Delta L_{4,P4}^{(em)}$	0.000 054 2 (13)
		$\Delta\delta m_{4,P4}^{(em)}$	0.000 878 6 (15)

4. *Muon g−2. Set III(a$_s$)*

The leading contribution to the muon $g-2$ comes from the case where both loops consist of electrons, namely the (mee) case, where m stands for the muon. Results of numerical evaluation in *Version A* are listed in Table X. From this Table and Table VI we obtain

$$a_\mu^{(10)}[\text{Set III(a}_s)^{(mee)}] = 43.048\ 8\ (194). \tag{41}$$

Next leading term is

$$a_\mu^{(10)}[\text{Set III(a}_s)^{(mem)}] = 12.190\ 3\ (176). \tag{42}$$

We also have

$$a_\mu^{(10)}[\text{Set III(a}_s)^{(met)}] \;=\; 0.469\ 43\ (39), \tag{43}$$

$$a_\mu^{(10)}[\text{Set III(a}_s)^{(mmt)}] \;=\; 0.150\ 11\ (21), \tag{44}$$

$$a_\mu^{(10)}[\text{Set III(a}_s)^{(mtt)}] \;=\; 0.013\ 68\ (3). \tag{45}$$

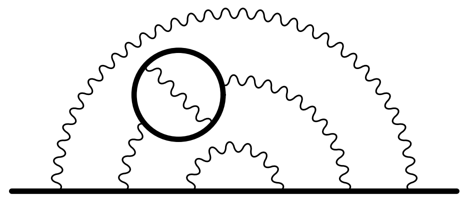

FIG. 4: Typical tenth-order diagrams of Set III(b) obtained by insertion of a fourth-order vacuum-polarization loop Π_4 in lepton diagrams of the three-photon-exchange type. Altogether there are 450 diagrams of this type.

These results are in good agreement with those of *Version B*.

III. SET III(B)

Diagrams belonging to this set are generated by inserting a proper fourth-order vacuum-polarization loop Π_4 (consisting of three diagrams) in the photon lines of M_6. Time-reversal invariance and use of the photon spectral function ρ_4 reduce the number of independent integrals from 450 to 8. These integrals are represented by the "self-energy-like" diagrams of Fig. 1. A typical diagram is shown in Fig. 4.

1. *Electron $g-2$: Version A*

Let $M_{6\alpha,P4}$ be the magnetic moment projection of the set of diagrams generated from a self-energy diagram α (=A through H) of Fig. 1 by insertion of Π_4 and an external vertex. The renormalized contribution due to the Set III(b) diagrams can then be written as

$$a_e^{(10)}[\text{Set III(b)} : \textit{Ver. A}] = \sum_{\alpha=A}^{H} a_{6\alpha,P4}, \tag{46}$$

with

$$a_{6\alpha,P4} = \Delta M_{6\alpha,P4} + \text{residual renormalization terms}, \tag{47}$$

where all divergences, except those within Π_4, are removed by intermediate renormalization by K_S and I_R operations. (See Ref. [32].)

The numerical values of Set III(b) integrals are summarized in Table XII. Numerical values of auxiliary integrals needed to complete the renormalization are listed in Table XIII.

TABLE XII: *Version A* contributions of Set III(b) diagrams to the electron $g-2$. n_F is the number of Feynman diagrams represented by the integral. All integrals are evaluated in double precision.

Integral	n_F	Value (Error) including n_F	Sampling per iteration	No. of iterations
$\Delta M_{6A,P4}$	15	−1.275 23 (8)	$1 \times 10^8, 1 \times 10^9$	50,50
$\Delta M_{6B,P4}$	15	1.865 05 (14)	$1 \times 10^8, 1 \times 10^9$	50,50
$\Delta M_{6C,P4}$	15	1.593 72 (14)	$1 \times 10^8, 1 \times 10^9$	50,50
$\Delta M_{6D,P4}$	30	1.166 99 (14)	$1 \times 10^8, 1 \times 10^9$	50,50
$\Delta M_{6E,P4}$	15	1.212 50 (6)	$1 \times 10^8, 1 \times 10^9$	50,50
$\Delta M_{6F,P4}$	15	1.113 25 (14)	$1 \times 10^8, 1 \times 10^9$	50,50
$\Delta M_{6G,P4}$	30	2.948 70 (24)	$1 \times 10^8, 1 \times 10^9$	50,50
$\Delta M_{6H,P4}$	15	−2.231 76 (22)	$1 \times 10^8, 1 \times 10^9$	50,50

When summed over all the diagrams of Set III(b), the UV- and IR-divergent pieces cancel out and the total contribution to $a^{(10)}$ can be written as a sum of finite pieces (which is similar to Eq. (5.39) of Ref. [32]):

$$\begin{aligned} a_e^{(10)}[\text{Set III(b)} : \textit{Ver. A}] = &\sum_{\alpha=A}^{H} \Delta M_{6\alpha,P4} \\ &- 3\Delta B_{2,P4}\Delta M_4 - 3\Delta B_2 \Delta M_{4,P4} \\ &+ \Delta\delta m_4 (M_{2^*,P4}[I] - M_{2^*,P4}) + \Delta\delta m_{4,P4}(M_{2^*}[I] - M_{2^*}) \\ &- [\Delta B_4 + 2\Delta L_4 - 2(\Delta B_2)^2] M_{2,P4} \\ &- [\Delta B_{4,P4} + 2\Delta L_{4,P4} - 4\Delta B_2 \Delta B_{2,P4}] M_2. \end{aligned} \tag{48}$$

Terms with suffix P_4 in Eq. (48) are obtained by insertion of Π_4 in the photon lines of diagrams. Note that K-operation is not applied to Π_4 so that we have $M_{2,P4}$, instead of $\Delta M_{2,P4}$, in Eq. (48).

Substituting the values listed in Tables XII and XIII into Eq. (48), we obtain

$$a_e^{(10)}[\text{Set III(b)} : \textit{Ver. A}] = 3.327\ 14\ (56). \tag{49}$$

TABLE XIII: Auxiliary integrals for the Set III(b). Some integrals are known exactly. Other integrals are obtained by VEGAS integration.

Integral	Value(Error)	Integral	Value(Error)
M_2	0.5	$M_{2,P4}$	0.052 870 652...
M_{2^*}	1.0	$M_{2^*,P4}$	0.145 597 (21)
$M_{2^*}[I]$	−1.0	$M_{2^*,P4}[I]$	−0.016 526 (69)
ΔM_4	0.030 833 612...	$\Delta M_{4,P4}$	−0.288 997 (12)
$\Delta\delta m_4$	1.906 340 (21)	$\Delta\delta m_{4,P4}$	1.773 79 (26)
ΔB_2	0.75	$\Delta B_{2,P4}$	0.183 666 8 (18)
ΔB_4	−0.437 094 (21)	$\Delta B_{4,P4}$	−0.816 23 (25)
ΔL_4	0.465 024 (17)	$\Delta L_{4,P4}$	0.559 72 (25)

2. *Electron g−2: Version B*

Let us now treat Set III(b) by the method based on the automated code generation scheme. In this approach, the contribution from Set III(b) is expressed as

$$\begin{aligned} a_e^{(10)}[\text{Set III(b)} : \textit{Ver. B}] = & \sum_{\alpha=A}^{H} \Delta M_{6\alpha,P4}^{(B)} \\ & - 3\Delta B_2 \Delta M_{4,P4} - 3\Delta B_{2,P4}\Delta M_4 \\ & - (\Delta B_4 + \Delta L_4 - 2(\Delta B_2)^2) M_{2,P4} \\ & - (\Delta B_{4,P4} + \Delta L_{4,P4} - 4\Delta B_2 \Delta B_{2,P4}) M_2, \end{aligned} \tag{50}$$

where

$$
\begin{aligned}
\Delta M^{(B)}_{6A,P4} &= \Delta M^{(A)}_{6A,P4} - 2\Delta L_{4b,1} M_{2,P4} - 2\Delta L_{4b,1,P4} M_2, \\
\Delta M^{(B)}_{6B,P4} &= \Delta M^{(A)}_{6B,P4} - \Delta L_{4b,2} M_{2,P4} - \Delta L_{4b,2,P4} M_2 \\
&- \Delta\delta m_{4b}(M_{2^*P4} - M_{2^*P4}[I]) - \Delta\delta m_{4b,P4}(M_{2^*} - M_{2^*}[I]), \\
\Delta M^{(B)}_{6C,P4} &= \Delta M^{(A)}_{6C,P4} - \Delta\delta m_{4a}(M_{2^*P4} - M_{2^*P4}[I]) \\
&- \Delta\delta m_{4a,P4}(M_{2^*} - M_{2^*}[I]), \\
\Delta M^{(B)}_{6D,P4} &= \Delta M^{(A)}_{6D,P4} - 2\Delta L_{4a,1} M_{2,P4} - 2\Delta L_{4a,1,P4} M_2, \\
\Delta M^{(B)}_{6E,P4} &= \Delta M^{(A)}_{6E,P4} - \Delta L_{4b,2} M_{2,P4} - \Delta L_{4b,2,P4} M_2, \\
\Delta M^{(B)}_{6F,P4} &= \Delta M^{(A)}_{6F,P4}, \\
\Delta M^{(B)}_{6G,P4} &= \Delta M^{(A)}_{6G,P4}, \\
\Delta M^{(B)}_{6H,P4} &= \Delta M^{(A)}_{6H,P4}.
\end{aligned}
\tag{51}
$$

Using the code generator we obtained the programs of the magnetic moments $M_{6\alpha,P4}$, $\alpha = A, \ldots, H$, and $M_{4\alpha}$, $M_{4\alpha,P4}$, $\alpha = A, B$. The programs for the renormalization constants $L_{4\alpha,P4}$, $L_{4\alpha}$, $B_{4\alpha,P4}$, $B_{4\alpha}$, $\delta m_{4\alpha,P4}$, $\delta m_{4\alpha}$ are also automatically generated. Other quantities, $\Delta B_{2,P4}$, $M_{2,P4}$ are very simple so that they are calculated by using hand-written programs. The values of ΔB_2 and M_2 are analytically known.

The results of numerical integration by VEGAS are shown in Table XIV.

Substituting the numbers shown in Tables XIV and XIII into Eq. (50), we obtain

$$
a_e^{(10)}[\text{Set III(b)} : \textit{Ver. B}] = 3.327\ 07\ (78) \tag{52}
$$

in good agreement with (49), where the uncertainty is from the numerical integration only.

TABLE XIV: *Version B* contributions of Set III(b) diagrams to the electron $g-2$. Programs are created by GENCODEN. n_F is the number of Feynman diagrams represented by the integral. All integrals are evaluated in double precision.

Integral	n_F	Value (Error) including n_F	Sampling per iteration	No. of iterations
$\Delta M_{6A,P4}$	15	$-1.673\ 94\ (34)$	$1\times 10^8, 1\times 10^9$	50, 50
$\Delta M_{6B,P4}$	15	$-0.959\ 45\ (24)$	$1\times 10^8, 1\times 10^9$	50, 50
$\Delta M_{6C,P4}$	15	$0.427\ 34\ (21)$	$1\times 10^8, 1\times 10^9$	50, 50
$\Delta M_{6D,P4}$	30	$1.110\ 10\ (32)$	$1\times 10^8, 1\times 10^9$	50, 50
$\Delta M_{6E,P4}$	15	$1.498\ 03\ (18)$	$1\times 10^8, 1\times 10^9$	50, 50
$\Delta M_{6F,P4}$	15	$1.113\ 12\ (20)$	$1\times 10^8, 1\times 10^9$	50, 50
$\Delta M_{6G,P4}$	30	$2.947\ 48\ (36)$	$1\times 10^8, 1\times 10^9$	50, 50
$\Delta M_{6H,P4}$	15	$-2.231\ 66\ (28)$	$1\times 10^8, 1\times 10^9$	50, 50

3. Mass-dependent terms A_2 of Set III(b)

The residual renormalization scheme (in *Version A*) for the (em) term is the following:

$$\begin{aligned} a_e^{(10)}[\text{Set III(b)}^{(em)}] = & \sum_{\alpha=A}^{H} \Delta M_{6\alpha,P4}^{(em)} \\ & - 3\Delta B_{2,P4}^{(em)} \Delta M_4 - 3\Delta B_2 \Delta M_{4,P4}^{(em)} \\ & + \Delta\delta m_4 (M_{2^*,P4}[I]^{(em)} - M_{2^*,P4}^{(em)}) + \Delta\delta m_{4,P4}^{(em)} (M_{2^*}[I] - M_{2^*}) \\ & - [\Delta B_4 + 2\Delta L_4 - 2(\Delta B_2)^2] M_{2,P4}^{(em)} \\ & - [\Delta B_{4,P4}^{(em)} + 2\Delta L_{4,P4}^{(em)} - 4\Delta B_2 \Delta B_{2,P4}^{(em)}] M_2. \end{aligned} \tag{53}$$

Substituting the values listed in Tables XI and XV into Eq. (53), we obtain

$$a_e^{(10)}[\text{Set III(b)}^{(em)}] = 0.002\ 794\ (1). \tag{54}$$

It is easy to obtain the contribution of tau lepton loop instead of the muon loop. We have simply to replace the muon mass by the tau mass in the FORTRAN programs. For instance a crude calculation in *Version A* yields

$$a_e^{(10)}[\text{Set III(b)}^{(et)}] = 0.000\ 021\ 42\ (1), \tag{55}$$

which is two orders of magnitude smaller than (54).

TABLE XV: Contributions of (em) diagrams of Fig. 2 to the Set III(b). n_F is the number of Feynman diagrams represented by the integral. All integrals are evaluated in double precision.

Integral	n_F	Value (Error) including n_F	Sampling per iteration	No. of iterations
$\Delta M_{6A,P4}^{(em)}$	15	$-0.000\ 389\ (\ 2)$	1×10^7	20
$\Delta M_{6B,P4}^{(em)}$	15	$0.000\ 943\ (\ 6)$	1×10^7	20
$\Delta M_{6C,P4}^{(em)}$	15	$0.000\ 925\ (\ 6)$	1×10^7	20
$\Delta M_{6D,P4}^{(em)}$	30	$0.000\ 592\ (\ 4)$	1×10^7	20
$\Delta M_{6E,P4}^{(em)}$	15	$0.000\ 371\ (\ 4)$	1×10^7	20
$\Delta M_{6F,P4}^{(em)}$	15	$0.000\ 773\ (\ 7)$	1×10^7	40
$\Delta M_{6G,P4}^{(em)}$	30	$0.001\ 626\ (26)$	1×10^7	60
$\Delta M_{6H,P4}^{(em)}$	15	$-0.000\ 751\ (20)$	1×10^7	20

4. Muon g−2. Set III(b)

The leading contribution to the muon $g-2$ comes from the case containing an electron loop, namely the (me) case, where m stands for the muon. Results of numerical evaluation (*Version A*) are listed in Table XVI. From this Table and Table XVII we obtain

$$a_\mu^{(10)}[\text{Set III(b)}^{(me)}] = 11.936\ 7\ (45). \tag{56}$$

We also obtained (*Version A*)

$$a_\mu^{(10)}[\text{Set III(b)}^{(mt)}] = 0.143\ 60\ (1). \tag{57}$$

These results are confirmed by *Version B* calculation.

IV. DISCUSSION

As was noted earlier *Version A* and *Version B* differ in the treatment of self-energy subtraction and IR divergence. Furthermore, the actual algebraic form of integrands in the first method [29] is quite different from the second one because "Kirchhoff's laws" satisfied by the scalar currents [32] were used extensively to make the integrand as compact as possible to save the computing time. Thus the two calculations can be regarded as independent

TABLE XVI: Contributions of (me)-type diagrams of Set III(b) to the muon $g-2$. n_F is the number of Feynman diagrams represented by the integral. All integrals are evaluated using the real(10) arithmetic built in *gfortran*.

Integral	n_F	Value (Error) including n_F	Sampling per iteration	No. of iterations
$\Delta M_{6A,P4}^{(me)}$	15	-16.0005 (53)	1×10^7	600
$\Delta M_{6B,P4}^{(me)}$	15	25.3670 (61)	1×10^7	900
$\Delta M_{6C,P4}^{(me)}$	15	2.8871 (61)	1×10^7	900
$\Delta M_{6D,P4}^{(me)}$	30	12.8166 (79)	1×10^7	1000
$\Delta M_{6E,P4}^{(me)}$	15	13.6292 (44)	1×10^7	600
$\Delta M_{6F,P4}^{(me)}$	15	6.9195 (59)	1×10^7	600
$\Delta M_{6G,P4}^{(me)}$	30	24.6728 (59)	1×10^7	700
$\Delta M_{6H,P4}^{(me)}$	15	-23.0066 (57)	1×10^7	800

TABLE XVII: Auxiliary integrals for the Set III(b)$^{(me)}$. Some integrals are known exactly. Other integrals are obtained by VEGAS integration.

Integral	Value(Error)	Integral	Value(Error)
M_2	0.5	$M_{2,P4}^{(me)}$	1.493 651 (84)
M_{2^*}	1.0	$M_{2^*,P4}^{(me)}$	3.122 88 (16)
$M_{2^*}[I]$	-1.0	$M_{2^*,P4}^{(me)}[I]$	-2.996 76 (24)
ΔM_4	0.030 833 612...	$\Delta M_{4,P4}^{(me)}$	-0.438 76 (26)
$\Delta\delta m_4$	1.906 340 (21)	$\Delta\delta m_{4,P4}^{(me)}$	13.651 22 (80)
ΔB_2	0.75	$\Delta B_{2,P4}^{(me)}$	2.439 109 (53)
ΔB_4	-0.437 094 (21)	$\Delta B_{4,P4}^{(me)}$	-3.826 32 (71)
ΔL_4	0.465 024 (17)	$\Delta L_{4,P4}^{(me)}$	3.653 31 (42)

of each other and the results agree within their error bars. Thus they may be combined statistically to yield the values listed below:

$$a_e^{(10)}[\text{Set III(a}_d)] = 0.9419\ (1), \tag{58}$$

$$a_e^{(10)}[\text{Set III(a}_s)] = 1.1854\ (2), \tag{59}$$

$$a_e^{(10)}[\text{Set III(b)}] = 3.3271\ (5). \tag{60}$$

The mass-dependent contribution of Set III(a_d) to the electron $g-2$, the sum of (22), (23), (24), and (25), is given by

$$a_e^{(10)}[\text{Set III}(\text{a}_d)(\text{mass-dep})] = 0.003\ 28\ (1), \tag{61}$$

while the mass-dependent contributions of Set III(a_s) to a_e is the sum of (37), (38), (39), and (40):

$$a_e^{(10)}[\text{Set III}(\text{a}_s)(\text{mass-dep})] = 0.004\ 32\ (10). \tag{62}$$

The total contribution of Set III(a) to a_e is the sum of (58), (59), (61), (62):

$$a_e^{(10)}[\text{Set III(a) (all terms)}] = 2.1349\ (2). \tag{63}$$

Similarly, from (54), (55), and (60) we obtain

$$a_e^{(10)}[\text{Set III(b) (all terms)}] = 3.3299\ (5). \tag{64}$$

The total contribution of Set III(a_d) to the muon $g-2$, the sum of (26), (27), (28), (29), (30), and (58), is

$$a_\mu^{(10)}[\text{Set III}(\text{a}_d)(\text{all terms})] = 55.360\ (19), \tag{65}$$

while the total contribution of Set III(a_s) to the muon g–2, the sum of (41), (42), (43), (44), (45), and (59), is

$$a_\mu^{(10)}[\text{Set III}(\text{a}_s)(\text{all terms})] = 57.058\ (26). \tag{66}$$

The total contribution of Set III(a) to the muon $g-2$, the sum of (65) and (66), is thus

$$a_\mu^{(10)}[\text{Set III(a)(all terms)}] = 112.418\ (32). \tag{67}$$

The total contribution of Set III(b) to the muon $g-2$, from (56), (57), and (60), is

$$a_\mu^{(10)}[\text{Set III(b)(all terms)}] = 15.4074\ (45). \tag{68}$$

The contribution of Set III(a) to the muon $g-2$ is very large, which is not unexpected. In particular, the orders of magnitude of contributions from the dominant (mee) terms of Set III(a_d) and Set III(a_s), as well as the (me) term of Set III(b), can be estimated crudely since their leading $log(m_\mu/m_e)$ term is determined by the renormalization procedure [3, 40]:

$$\begin{aligned}
a_\mu^{(10)}[\text{Set III}(\text{a}_d)^{(mee)}] &\sim 3K_2^2 a_e^{(6)}(\textit{no loop}) \sim 34, \\
a_\mu^{(10)}[\text{Set III}(\text{a}_s)^{(mee)}] &\sim 3K_{2,2} a_e^{(6)}(\textit{no loop}) \sim 34, \\
a_\mu^{(10)}[\text{Set III(b)}^{(me)}] &\sim 3K_4 a_e^{(6)}(\textit{no loop}) \sim 7,
\end{aligned} \tag{69}$$

with

$$
\begin{aligned}
K_2 &\sim \frac{2}{3}\ln(m_\mu/m_e) - ...,\\
K_{2,2} &\sim K_2^2,\\
K_4 &\sim \frac{1}{2}\ln(m_\mu/m_e) - ...,
\end{aligned}
\tag{70}
$$

and [30]

$$
a_e^{(6)}(\textit{no loop}) = 0.904\ 979\ ....,
\tag{71}
$$

where *no loop* means diagrams without closed lepton loops of vacuum-polarization type. The factor 3 accounts for the increase in the number of diagrams caused by insertion of vacuum-polarization loops. As is expected from (69) and (70), the values of (26) and (41) are of the same order of magnitude.

Acknowledgments

This work is supported in part by the JSPS Grant-in-Aid for Scientific Research (C)19540322, (C)20540261, and (C)23540331. The part of material presented by T. K. is based on work supported by the U. S. National Science Foundation under the Grant NSF-PHY-0757868, and the International Exchange Support Grants (FY2010) of RIKEN. T. K. thanks RIKEN for the hospitality extended to him while a part of this work was carried out. Numerical calculations are conducted on the RIKEN Supercombined Cluster System (RSCC) and the RIKEN Integrated Cluster of Clusters (RICC) supercomputing systems.

---

[1] D. Hanneke, S. Fogwell, and G. Gabrielse, Phys. Rev. Lett. **100**, 120801 (2008).

[2] D. Hanneke, S. Fogwell Hoogerheide, and G. Gabrielse, arXiv:1009.4831 [physics.atom-ph].

[3] T. Kinoshita and M. Nio, Phys. Rev. D **73**, 053007 (2006).

[4] T. Aoyama, M. Hayakawa, T. Kinoshita, and M. Nio, Phys. Rev. Lett. **99**, 110406 (2007).

[5] T. Aoyama, M. Hayakawa, T. Kinoshita, and M. Nio, Phys. Rev. D **77**, 053012 (2008).

[6] M. Davier, A. Höcker, B. Malaescu, and Z. Zhang, Eur.Phys.J. **C71**, 1515 (2010).

[7] T. Teubner, K. Hagiwara, R. Liao, A. D. Martin, and D. Nomura, arXiv:1001.5401 [hep-ph].

[8] B. Krause, Phys. Lett. **B390**, 392 (1997).

[9] K. Melnikov and A. Vainshtein, Phys. Rev. D **70**, 113006 (2004).

[10] J. Bijnens and J. Prades, Mod. Phys. Lett. **A22**, 767 (2007).

[11] J. Prades, E. de Rafael, and A. Vainshtein, arXiv:0901.0306 [hep-ph].

[12] A. Nyffeler, Phys. Rev. D **79**, 073012 (2009).

[13] A. Czarnecki, B. Krause, and W. J. Marciano, Phys. Rev. Lett. **76**, 3267 (1996).

[14] M. Knecht, S. Peris, M. Perrottet, and E. de Rafael, J. High Energy Phys. **11**, 003 (2002).

[15] A. Czarnecki, W. J. Marciano, and A. Vainshtein, Phys. Rev. D **67**, 073006 (2003), **73**, 119901(E) (2006).

[16] R. Bouchendira, P. Clade, S. Guellati-Khelifa, F. Nez, and F. Biraben, Phys.Rev.Lett. **106**, 080801 (2011).

[17] P. J. Mohr, B. N. Taylor, and D. B. Newell, Rev. Mod. Phys. **80**, 633 (2008).

[18] T. Kinoshita and M. Nio, Phys. Rev. D **70**, 113001 (2004).

[19] T. Aoyama, M. Hayakawa, T. Kinoshita, and M. Nio, Nucl. Phys. **B740**, 138 (2006).

[20] T. Aoyama, M. Hayakawa, T. Kinoshita, and M. Nio, Nucl. Phys. **B796**, 184 (2008).

[21] T. Aoyama, M. Hayakawa, T. Kinoshita, M. Nio, and N. Watanabe, Phys. Rev. D **78**, 053005 (2008).

[22] T. Aoyama, M. Hayakawa, T. Kinoshita, and M. Nio, Phys. Rev. D **78**, 113006 (2008).

[23] T. Aoyama, K. Asano, M. Hayakawa, T. Kinoshita, M. Nio, and N. Watanabe, Phys. Rev. D **81**, 053009 (2010).

[24] T. Aoyama, M. Hayakawa, T. Kinoshita, and M. Nio, Phys. Rev. D **82**, 113004 (2010).

[25] T. Aoyama, M. Hayakawa, T. Kinoshita, and M. Nio, Phys.Rev. **D83**, 053003 (2011).

[26] T. Aoyama, M. Hayakawa, T. Kinoshita, and M. Nio, Phys.Rev. **D83**, 053002 (2011).

[27] S. Laporta, Phys. Lett. **B328**, 522 (1994).

[28] J.-P. Aguilar, E. de Rafael, and D. Greynat, Phys.Rev. **D77**, 093010 (2008).

[29] P. Cvitanović and T. Kinoshita, Phys. Rev. D **10**, 3978 (1974).

[30] S. Laporta and E. Remiddi, Phys. Lett. **B379**, 283 (1996).

[31] A. O. G. Kallen and A. Sabry, Kong. Dan. Vid. Sel. Mat. Fys. Med. **29N17**, 1 (1955).

[32] T. Kinoshita, in *Quantum electrodynamics*, edited by T. Kinoshita (World Scientific, Singapore, 1990), pp. 218–321, (Advanced series on directions in high energy physics, 7).

[33] P. Cvitanović and T. Kinoshita, Phys. Rev. D **10**, 3991 (1974).

[34] G. P. Lepage, J. Comput. Phys. **27**, 192 (1978).

[35] T. Kinoshita and W. B. Lindquist, Phys. Rev. Lett. **47**, 1573 (1981).

[36] T. Kinoshita and M. Nio, Phys. Rev. D **60**, 053008 (1999).

[37] M. Passera, Phys. Rev. D **75**, 013002 (2007).

[38] S. Laporta, Nuovo Cim. **A106**, 675 (1993).

[39] H. Elend, Phys. Lett. **20**, 682 (1966).

[40] T. Kinoshita, Nuovo Cimento B **51**, 140 (1967).